Coordinated Science Laboratory

UNIVERSITY OF ILLINOIS - URBANA, ILLINOIS

ATOMIC PROCESSES IN HELIUM-KRYPTON AND HELIUM-XENON MIXTURES

C.L. Chen

REPORT R-171 JUNE, 1963

COORDINATED SCIENCE LABORATORY
UNIVERSITY OF ILLINOIS
URBANA, ILLINOIS

Contract DA-36-039-TR US AMC 02208(E)
DA Project 3A-99-25-004

The research reported in this document was made possible by support extended to the University of Illinois, Coordinated Science Laboratory, jointly by the Department of the Army, Department of the Navy (Office of Naval Research), and the Department of the Air Force (Office of Scientific Research) under Department of Army Contract DA-36-039-TR US AMC 02208(E).

ABSTRACT

The momentum transfer collision frequency of thermal electrons with neutrals in a decaying plasma established in helium-krypton and helium-xenon mixtures of known proportions were measured by microwave interferometer at gas temperatures of $\sim$ 200 to 600°K. The energy dependences of the momentum transfer cross sections of electrons with krypton and xenon atoms deduced from these measurements are best represented by:
$Q_m(u) = 6.56 \times 10^{-15} - 2.79 \times 10^{-14} u^{\frac{1}{2}} + 3.14 \times 10^{-14} u$ and
$1.91 \times 10^{-14} - 8.30 \times 10^{-14} u^{\frac{1}{2}} + 9.40 \times 10^{-14} u\ cm^2$, respectively. Here u is the electron energy in electron volts. Mobilities of Kr^+ and Xe^+ in helium and in their respective parent gas have also been determined, from the characteristic time constants of the electron density decay measured in the afterglow in the mixtures at low pressures, to be: $\mu(Kr^+$ in He$)$ = 2.02 ± 1.2 cm^2/volt-sec, $\mu(Kr^+$ in Kr$) = 1.01 \pm 0.06$, $\mu(Xe^+$ in He$) = 18 \pm 1.1$ and $\mu(Xe^+$ in Xe$) = 0.55 \pm 0.03$ at $\sim$ 300°K. A study of the pressure dependence of the characteristic time constants of the electron density decay at fixed ratios of krypton to helium and xenon to helium concentrations yields the three body conversion frequency of atomic krypton and xenon ions to their respective molecular ions.

I. INTRODUCTION

The employment of microwave technology in studying the fundamental atomic collision processes in a weakly ionized gas is well known.[1] Nevertheless, questions have been occasionally raised as to the assumption of thermal equilibrium of the electron gas with the neutrals at times in the afterglow the experiment was performed. In some cases, evidences showed that the electron temperature did sustain at a level above that of the neutrals at times several hundred microseconds to a few milliseconds after removal of the excitation source. Since almost all physical parameters determined by microwave methods are related directly or indirectly to the electron temperature, it would be appropriate that the electron temperature is measured experimentally. In the present communication, the complete thermalization of the electrons with the neutrals in He-Kr and He-Xe mixtures is demonstrated by a comparison of the microwave noise emitted from the plasma with that of a standard noise source as detected by a ruby maser. One of the reasons for mixing krypton and xenon with helium is to utilize the helium as a "recoil" gas for the electrons. Quantitative and qualitative descriptions of various collisional processes are then obtained from the measurements made in the afterglow established in such mixtures. The problems of interest are: (1) the energy dependence of the momentum transfer cross sections of electrons with krypton and xenon atoms at energies below Ramsauer minimum; (2) the mobilities of thermal Kr^+ and Xe^+ ions in helium and in their respective parent gas at room temperature (i.e. $\sim 300^oK$); (3) the conversion frequency ν_{conv} of atomic krypton and xenon ions to molecular ions according to the three-body process[2]

$$\begin{matrix} Kr^+ \\ + \\ Xe^+ \end{matrix} \quad \begin{matrix} Kr \\ + \\ Xe \end{matrix} \; + He \rightarrow \begin{matrix} Kr_2^+ \\ \\ Xe_2^+ \end{matrix} \; + He$$

and (4) some qualitative evidence in supporting a suggested process of molecular krypton ions formation, through collisions of high-lying, short-lived excited atoms with ground state atoms,

$$Kr^* + Kr \rightarrow Kr_2^+ + e$$

by Hornbeck and Molnar.[3]

II. EXPERIMENTAL APPARATUS

The gas handling system is of standard high vacuum type[4] baked at $\sim 400^{\circ}C$ for more than 24 hours prior to each sequence of experiments. An ultimate vacuum of the order of 2 to 6×10^{-10} mmHg is attained. Gases are then introduced into the discharge tube, and the pressure is measured by a (capacity) null reading manometer.[5] The gases used are mass spectrometer controlled grade supplied from Linde Air Products Company. The discharge tube is made of thin wall (0.7 mm thick) pyrex tubing of 22 mm outside diameter and 72 cm long with 6 cm tapering to a point at each end. The tube is housed coaxially in a one inch by one inch square waveguide which is connected to the standard x-band waveguide system through two six inch tapering sections. The gas is ionized by a variable high voltage dc pulse of several thousand volts and seven microseconds duration repeated at a frequency of 31.2 cycles per sec. The electrodes of the discharge tube are made out of high purity titanium for its good gettering property for the atmospheric gases.[6] Electron density variations and the effective electron collision frequency ν_{eff} for momentum transfer are measured by microwave interferometry in the decaying plasma created in helium-krypton and helium-xenon mixtures. A schematic diagram of the microwave circuitry used in part of the experiment is shown in Figure 1. A low power ($\sim 2\ \mu w$), 9.03 or 8.53 kMc/sec probing signal (continuous or pulsed) is employed to measure the phase shifts and attenuations on the microwave due to the presence of plasma. The temperature of the discharge tube is monitored constantly by three copper-constantan thermocouples.

III. MOMENTUM TRANSFER COLLISION CROSS SECTION

Margenau[7] has shown that the electrical conductivity σ_c of a weakly ionized gas under the action of a low level rf field is given by

$$\sigma_c = \sigma_r + j\sigma_i = - \frac{ne^2}{3m} \int \frac{v \frac{\partial f_o}{\partial v}}{\nu + j\omega} d^3v \qquad (1)$$

where σ_r and σ_i are the real and imaginary parts of σ_c. m is the electron mass, e the electron charge, n the electron density and v the electron velocity. ω is the radian frequency of the applied electric field. $\nu = \sum_i N_{m_i} Q_{m_i} (v)v$ is the momentum transfer collision frequency of the electrons with all species in the plasma. Here N_{m_i} is the density of the i^{th} species. In the case of $\omega^2 \gg \nu^2$ and the electron velocity distribution function to be independent of the proportion of the gas mixture and furthermore f_o (the zeroth order spherical harmonic expansion of the electron velocity distribution function) to be maxwellian,

$$\sigma_r = \frac{ne^2}{m\omega^2} \nu_{eff} \qquad (2)$$

where

$$\nu_{eff} = \nu_{em_1} + \nu_{em_2} + \nu_{ei} \tag{3}$$

is the effective electron collision frequency for momentum transfer. ν_{em_1}, ν_{em_2} are the electron collision frequencies with gas species 1 and 2, respectively, and

$$\nu_{em_i} = \frac{N_{m_i}}{3} \left(\frac{2}{\pi}\right)^{\frac{1}{2}} \left(\frac{m}{kT_e}\right)^{5/2} \int_0^{\infty} Q_{m_i}(v) v^5 \exp\left[-\frac{mv^2}{2kT_e}\right] dv \tag{4}$$

i = 1, 2. k is the Boltzmann's constant and T_e the electron temperature. $Q_{m_i}(v)$ is the momentum transfer collision cross section of electrons with $i^{\underline{th}}$ species of atom and is defined[8] as

$$Q_{m_i}(v) = \int (1 - \cos\theta) I(\theta,v) d\Omega$$

where $I(\theta,v)$ is the differential scattering cross section for a scattering angle θ and relative velocity v.[9] ν_{ei} is the electron-ion collision frequency and is represented by[10]

$$\nu_{ei} = 3.59 \frac{N_i}{T_e^{3/2}} \ell n \frac{3.32 \times 10^3 T_e^{3/2}}{N_i^{\frac{1}{2}}} \tag{5}$$

where N_i is the ion density. In our experiments, ν_{ei}/ν_{eff} is of the order of 1 to 10% in the afterglow in which ν_{eff} is measured. If we define $\nu_{em} = \nu_{em_1} + \nu_{em_2}$, then it is easily shown that

$$\frac{\nu_{em}}{p_t} = \left[\frac{\nu_{em_1}}{p_1} - \frac{\nu_{em_2}}{p_2}\right] \frac{p_1}{p_t} + \frac{\nu_{em_2}}{p_2} \tag{6}$$

where p_t is the total gas pressure and is equal to the sum of the partial pressures p_1 and p_2 of the mixtures. All pressures are hereafter referred to 0^oC. Therefore, the ratio of measured electron-molecule collision frequency to the total gas pressure is a linear function of fractional concentration of gas 1 at a fixed temperature. ν_{em_1}/p_1 and ν_{em_2}/p_2 are determined from the intersections at $p_1/p_t = 1$ and 0, respectively. $Q_{m_1}(v)$ can then be determined experimentally from Eq (4) should there be enough data of ν_{em_1}/p_1 as a function of temperature is provided.

IV. ION MOBILITIES AND CONVERSION FREQUENCIES

The main electron loss process in the afterglow of a low pressure, weakly ionized noble gaseous discharge is ambipolar diffusion.[11] For the present experiments (helium-krypton or helium-xenon mixtures of various proportions) the ions created in the active discharge are believed to be atomic krypton or xenon ions when suitable breakdown voltage pulse is employed.[12] This is supported by the spectral examination of the discharge in He-Kr mixtures with a Bausch and Lomb Littrow No. 5402 Spectrograph which has a dispersion of 7.7 A/mm at 3670 A and 45.5 A/mm at 6700 A. It is found that no band spectra of any kind and only atomic krypton lines are presented. Hornbeck and Molnar[3] noticed in their mass spectrometric studies of molecular ions in noble gases that Kr_2^+ and Xe_2^+ ions are much more difficult to be formed than He_2^+, Ne_2^+, and A_2^+ through a process suggested by them. At low gas pressures and careful breakdown conditions,[12] the molecular ion formation process proposed by Hornbeck and Molnar[3] can be ignored. However, another mechanism seems to be possible for their formation. That is, Kr^+ or Xe^+ ions, while traversing through the mixture to the walls in a decaying plasma, experience not only elastical scatterings from helium and their parent gas atoms, but also may change their identities to molecular ions through three-body collisions

$$\begin{matrix} Kr^+ \\ + \\ Xe^+ \end{matrix} \quad \begin{matrix} Kr \\ + \\ Xe \end{matrix} \; + \; He \rightarrow \begin{matrix} Kr_2^+ \\ + \\ Xe_2^+ \end{matrix} \; + \; He \tag{7}$$

The differential equations governing the decaying plasma are

$$\frac{\partial n_A}{\partial t} = D_{aA} \nabla^2 n_A - \nu_{conv} n_A \tag{8a}$$

$$\frac{\partial n_M}{\partial t} = D_{aM} \nabla^2 n_M + \nu_{conv} n_A \tag{8b}$$

and

$$n = n_A + n_M \tag{8c}$$

Here electron decay through recombinations has been neglected in this case for its ineffectiveness.[13] n_A and n_M are the number densities of the atomic and molecular ions, respectively. D_{aA} and D_{aM} are the ambipolar diffusion coefficients of the atomic and molecular ions in the mixtures and $\nu_{conv} = C_{conv} p_1 p_2$ is the atomic to molecular ion conversion frequency according to reaction (7). The conversion coefficient C_{conv} is a constant and is different for Kr^+ than for Xe^+. The set of equations is solved for the boundary conditions of zero densities for all constituents at the walls.

The solution for the electron density is

$$n(t) = n_A(0)\left[1 - \frac{\nu_{conv}}{\frac{1}{\tau_A} - \frac{1}{\tau_M}}\right]\exp\left[-\frac{t}{\tau_A}\right] + \left[n_M(0) + \frac{n_A(0)\nu_{conv}}{\frac{1}{\tau_A} - \frac{1}{\tau_M}}\right]\exp\left[-\frac{t}{\tau_M}\right] \tag{9}$$

where

$$\frac{1}{\tau_A} = \frac{D_{aA}}{\Lambda^2} + \nu_{conv} \tag{10}$$

and

$$\frac{1}{\tau_M} = \frac{D_{aM}}{\Lambda^2} \tag{11}$$

Λ is the characteristic diffusion length of the discharge tube. Since ν_{conv} is proportional to the square of the gas pressure, $\nu_{conv}\left[\frac{1}{\tau_A} - \frac{1}{\tau_M}\right]^{-1} << 1$ at low pressures. This together with the initial condition $n_M(0) \simeq 0$ (see section V) and the fact that $\tau_M < \tau_A$ (due principally to the lack of charge transfer process of the molecular ions with the neutrals) gives the final slope of ℓn n versus t plot to be $- \tau_A^{-1}$. It is easy to show from Eq (10) that the product of ambipolar diffusion coefficient D_a of electrons to the partial pressure of helium in the helium-krypton mixtures, for example, takes the following form

$$D_a p(He) = \frac{T_e}{7.63} \frac{\mu(Kr^+ \text{ in He})}{1 + \frac{p(Kr)}{p(He)} \frac{\mu(Kr^+ \text{ in He})}{\mu(Kr^+ \text{ in Kr})}} + \Lambda^2 C_{conv} p^2(He) p(Kr) \tag{12}$$

where $\mu(Kr^+$ in He) and $\mu(Kr^+$ in Kr) are the mobilities of atomic krypton ions in helium and in krypton, respectively, referred to 0^oC and 760 mmHg gas pressure. p(Kr) and p(He) are the partial pressures of krypton and helium in the mixtures. In deriving Eq (12), Einstein's relation[14]

$$D = \frac{kT}{e} \mu$$

and Blanc's law[15]

$$\frac{1}{\mu} = \frac{p(Kr)}{p_t} \frac{1}{\mu(Kr^+ \text{ in Kr})} + \frac{p(He)}{p_t} \frac{1}{\mu(Kr^+ \text{ in He})}$$

have been employed. Here μ is the mobility of Kr^+ ions in helium-krypton mixture. Mobilities of Kr^+ ions in helium and in krypton and the proportionality constant C_{conv} in the conversion frequency can be determined from a best fit of $D_a p(He)$ as a function of $p(Kr)/p(He)$ according to Eq (12). Similar treatment can be applied in the case of helium-xenon mixtures.

V. RESULTS AND DISCUSSIONS

One of the crucial parameters in studying atomic processes in a decaying plasma by microwave is the electron temperature. Radiometer[16] has been used in the past to study the electron temperature decay in an afterglow. Evidences[17] showed, in some cases, that electrons did sustain at a temperature much higher than that of the gas even several hundred microseconds in the post-discharge. To bring down the electron temperature to that of the gas quickly in the afterglow, Biondi[18] employed helium as a "recoil" gas. That helium gas is added to krypton and xenon in the present experiment is just for this purpose. The electron temperature relaxation after termination of the breakdown pulse in the present experiment is observed by a ruby maser operating at a pump frequency of $\sim$ 21 kMc/sec and a signal frequency of 8.53 kMc/sec to monitor the noise emanating from the discharge tube. A standard noise source is used for comparison. The maser has a gain of $\sim$25 db. A typical example is shown in Fig. 2. In this case, a plasma is created by a high voltage pulse in helium-xenon mixture of 54.6% xenon and a total pressure of 4.83 mmHg. The background gas temperature is 303°K. Fig. 2b is the picture of the transmitted microwave signal. It remains cut off up to 450 μsec in the afterglow. In this time interval, no reflection is detected and the absorptivity of the plasma is unity. A direct comparison of the noise emitted by the plasma with a standard noise source, as shown in Fig. 2a, indicates that the electron temperature has reached that of the gas approximately

300 μsec after termination of the pulse. Fig. 2c is the microwave interferometer trace from which the decay of electron density is calculated.

It is shown in Eq (6) that the ratio of total measured electron-molecule collision frequency to the gas pressure is a linear function of the fractional concentration of either gas in a binary mixture at constant temperature. This is confirmed in the experiments of He-Kr and He-Xe mixtures at 200 and 303°K, under the condition of $(\frac{\omega}{\nu})^2 \gg 1$ (usually $(\frac{\omega}{\nu})^2 \simeq 100$ in the present experiment). The results are shown in Figures 3 and 4. From the extrapolated values of ν_{em}/p_t at $p(Kr)/p_t$ and $p(Xe)/p_t = 0$ and 1, the momentum transfer collision probability $\overline{P}_m$[19] of electrons with He, Kr, and Xe atoms are calculated at these two temperatures. They are: 18.9, 54.7, and 151 cm^2/cm^3, respectively, at 303°K and 18.9, 77.5, and 221 cm^2/cm^3, respectively, at 200°K. Thus, within experimental accuracy, $\overline{P}_m(He)$ and hence $Q_m(v)$ for He is a constant in this range. This fact agrees with what has been found by other investigators[20] and is utilized later on in deducing $\nu_{em}(Kr)/p(Kr)$ and $\nu_{em}(Xe)/p(Xe)$ from ν_{eff}/p_t measured at higher temperatures. The temperature dependence of $\nu_{em}(He)/p(He)$ is taken to be

$$\frac{\nu_{em}(He)}{p(He)} = 1.56 \times 10^7 T_e^{\frac{1}{2}} \quad sec^{-1}\text{-mmHg}^{-1} \tag{13}$$

By subtracting electron-ion (as calculated from Eq (5)) and electron-helium (as calculated from Eq (13)) contributions from ν_{eff}, the resulting momentum transfer collision frequency of electrons with Kr and Xe atoms as a function of electron temperature is shown in Figures 5 and 6. The velocity dependence of the momentum transfer cross section $Q_m(v)$ is determined from a best fit to the experimental points according to Eq (4). In so doing, $Q_m(v)$ is assumed by a three term polynomial of the following form

$$Q_m(v) = A + Bv + Cv^2 \quad cm^2$$

The solid curves on Figures 5 and 6 are so found with

$$A = 6.56 \times 10^{-15} \quad cm^2$$

$$B = -4.70 \times 10^{-22} \quad cm\text{-}sec$$

$$C = 8.87 \times 10^{-30} \quad sec^2$$

for krypton and

$$A = 1.91 \times 10^{-14} \quad cm^2$$

$$B = -1.40 \times 10^{-21} \quad cm\text{-}sec$$

$$C = 2.67 \times 10^{-29} \quad sec^2$$

for xenon. Then the energy dependence of these cross sections can easily be shown to be

$$Q_m(u) = 6.56 \times 10^{-15} - 2.79 \times 10^{-14} u^{\frac{1}{2}} + 3.14 \times 10^{-14} u \quad cm^2 \qquad (14)$$

for krypton and

$$Q_m(u) = 1.91 \times 10^{-14} - 8.30 \times 10^{-14} u^{\frac{1}{2}} + 9.40 \times 10^{-14} u \quad cm^2 \qquad (15)$$

for xenon. Here u is the electron energy in electron volts.

Recently, Pack, Volshall and Phelps (PVP)[21] have deduced $Q_m(u)$ from their electron mobility studies in Kr and Xe. Their results, together with the present one, are shown in Figures 7 and 8. In which PVP's notations are preserved. O'Malley[22] has adopted "atomic effective range formulas"[23] to analyze Ramsauer-Kollath (RK) scattering experiments.[24] In this analysis, the parameters of the theory are so chosen to fit RK experimental cross sections. These calculations were extrapolated to zero energy and are shown in Figures 7 and 8. All agree fairly well with each other in shape but not in absolute value. The disagreements can be attributed partly to the approximations and experimental errors in each case.

In Section IV it is shown that at low gas pressures and suitable breakdown conditions the ultimate inverse characteristic time constant of the electron density decay is given by Eq (10) from which Eq (12) is derived. Since the second term to the right hand side of Eq (12) is proportional to the third power of the total gas pressure, and can be neglected at very low gas pressures, i.e.,

$$D_a p(\mathrm{He}) = \frac{T_e}{7.63} \frac{\mu(\mathrm{Kr}^+ \text{ in He})}{1 + \frac{p(\mathrm{Kr})}{p(\mathrm{He})} \frac{\mu(\mathrm{Kr}^+ \text{ in He})}{\mu(\mathrm{Kr}^+ \text{ in Kr})}} \tag{16}$$

$\mu(\mathrm{Kr}^+$ in He) and $\mu(\mathrm{Kr}^+$ in Kr) are then determined from the best fit of the measured quantities $D_a p(\mathrm{He})$ and $p(\mathrm{Kr})/p(\mathrm{He})$ at a constant temperature according to Eq (16). This is shown in Figure 9 and the results are: $\mu(\mathrm{Kr}^+$ in He) = 20.2 ± 1.2 cm^2/volt-sec and $\mu(\mathrm{Kr}^+$ in Kr) = 1.0 ± 0.06 at 303°K. Figure 10 shows the results in the case of He-Xe mixtures, the best fit gives: $\mu(\mathrm{Xe}^+$ in He) = 18 ± 1.1 and $\mu(\mathrm{Xe}^+$ in Xe) = 0.55 ± 0.03 at 303°K.

The theoretical calculated mobilities of thermal energy ion relevant to the present experiment, together with the values determined by other authors, are presented in Table I. The theoretical values of $\mu(\mathrm{Kr}^+$ in He) and $\mu(\mathrm{Xe}^+$ in He) are calculated by the use of Langevin's theory in the polarization limit.[25] The dielectric constant for helium adopted here is that recommended by Maryott and Buckley.[26]

A close examination of Eq (12) suggests that, for a fixed percentage of krypton (or xenon) in helium, the measured values of $D_a p(\mathrm{He})$ should vary linearly with $p^2(\mathrm{He})p(\mathrm{Kr})$ should there be the three-body molecular ion formation process. The slope of $D_a p(\mathrm{He})$ versus $p^2(\mathrm{He})p(\mathrm{Kr})$ yields the value of

$C_{conv}\Lambda^2$, and it is independent of the krypton percentage in helium. Figure 11 presents the results in four different krypton percentages, i.e., 1.7, 4.3, 5.97, and 14%. The slopes are fairly well the same, and C_{conv} so determined is (76 ± 4) $mmHg^{-2}\ sec^{-1}$ and

$$\nu_{conv} = (76 \pm 4)p(He)p(Kr)$$

Similar studies are also made for Xe^+ to Xe_2^+ conversion. Typical results are shown in Figure 12. In this case, C_{conv} = (140 ± 9) $mmHg^{-2}sec^{-1}$ and

$$\nu_{conv} = (140 \pm 9)p(He)p(Xe).$$

Similar to the gas-kinetic conditions[27] in two-body charge or excitation transfer collisions, it is reasonable to believe that the lesser the amount of energy carried away by the third body in reaction (7), the higher the probability of molecular ion formation. Then the larger value of C_{conv}, which is proportional to the probability, for Xe^+ to Xe_2^+ than Kr^+ to Kr_2^+ indicates that the amount of energy carried away by He is smaller in the former than in the latter case. Should this be so, the binding energy of Xe_2^+ would be smaller than that of Kr_2^+. This has to wait a further study in appearance potentials in these gases to confirm it. Nevertheless, observations by Hornbeck and Molnar[3] seemed to suggest the same explanation. They noticed, in their mass spectrometry studies of molecular ions formed by electron bombardment in noble gases, that the current peaks of Xe^+ to Xe_2^+ is 4×10^4 to 1 while Kr^+ to Kr_2^+ is 2×10^4 to 1. The apparent more difficulty in Xe_2^+ formation than Kr_2^+ through (taking xenon as an example)

$$e + Xe \rightarrow Xe^* + e \qquad (17a)$$

$$Xe^* + Xe \rightarrow Xe_2^+ + e \qquad (17b)$$

could be explained as that Xe^* (stands for xenon atom in a high-lying, short-lived excited state) required for the reaction must be very close to the ionization limit if the binding energy of Xe_2^+ were very small. The excitation cross section is known to drop off rapidly in general as the total quantum number increases.[27] Therefore, their finding seems to be in harmony with C_{conv} determined here.

We have also studied qualitatively the molecular ion formation processes proposed by Hornbeck and Molnar[3] [see Eqs (17a) and (17b)]. We observe (see Figures 13, 14) that the characteristic time constant of the electron density decay is a strong function of the excitation light in the active discharge, while keeping p_t and the relative concentration of Kr unchanged. Qualitatively, the brighter the excitation light (indicated in Figures 13 and 14 by the higher breakdown voltage pulse setting) the smaller the characteristic ambipolar diffusion time constant. Since electrons have already relaxed back to the gas temperature at times in the afterglow the measurements were made and high order modes of diffusion are believed not to exist at such late times in the afterglow. The only feasible explanation offered to such phenomenon is the formation of molecular ions through processes (17a) and (17b). Xe_2^+ or Kr_2^+ ions are known to have a higher mobility than Xe^+ or Kr^+ in their parent gases. The light intensity in the active discharge is interpreted as an indirect measure of Xe^* or Kr^* concentrations. No detailed correlations between the distribution of line intensities and the molecular ion concentrations are pursued at the present time. Further mass- and optical spectrometry studies are necessary.

ACKNOWLEDGEMENTS

It is a great pleasure to acknowledge Mr. P. D. Goldan of Gaseous Electronics Laboratory of this university for loaning his maser to and assisting the author in the afterglow noise measurements in part of the present investigation. The author is also indebted to his colleague, Dr. M. Raether, for many interesting and fruitful discussions and his careful reading of the manuscript.

Table I. Comparison of Experimental and Theoretical Values of Kr^+ and Xe^+ Mobilities (in cm^2/volt-sec).

Gas \ Ion / Mobility	Kr^+ Experiment	Kr^+ Theory	Xe^+ Experiment	Xe^+ Theory
He	20.2±1.2[a]	17.0	18 ± 1.1[a]	16.8
Kr	0.9-0.95[b] 0.90[c] 1.01±0.06[a]	1.0[d] 0.9[e]		
Xe			0.6-0.65[b] 0.58[c] 0.55±0.03[a]	0.66[d] 0.60[e]

a. Present data

b. R. N. Varney, Phys. Rev. 88, 362 (1952).

c. M. A. Biondi and L. M. Chanin, Phys. Rev. 94, 910 (1954).

d. I. B. Bernstein (unpublished).

e. A. Dalgarno, Phil. Trans. Roy. Soc. London A, 250, 426 (1958).

REFERENCES

1. The pertinent references can be found in the review articles of:
   L. Goldstein, Advances in Electronics and Electron Physics (Academic Press, Inc., New York 10, New York, 1955), Vol. VII, p. 473.
   S. C. Brown, Basic Data of Plasma Physics (The Technology Press of the Massachusetts Institute of Technology and John Wiley & Sons, Inc., New York, 1959).

2. This is similar to the three-body He_2^+ formation process studied by A. V. Phelps and S. C. Brown, Phys. Rev. 86, 102 (1952).

3. J. A. Hornbeck and J. P. Molnar, Phys. Rev 84, 621 (1951).

4. D. Alpert, J. Appl. Phys. 24, 860 (1953).

5. The design is originated from Westinghouse Research Laboratories, Pittsburgh, Pennsylvania. A unique package is now marketed by Granville-Phillips Company, Boulder, Colorado.

6. V. L. Stout and M. D. Gibbons, J. Appl. Phys. 26, 1488 (1955).

7. H. Margenau, Phys. Rev. 69, 508 (1946).

8. H. S. W. Massey and E. H. S. Burhop, Electronic and Ionic Impact Phenomena (Oxford at the Clarendon Press, 1952), p. 367.

9. Since the electron to molecule mass ratio is very small, the relative velocity of the electrons with the molecule can be approximated by the electron velocity alone, and no distinction in symbols for these two velocities are adopted here.

10. V. L. Ginsberg, J. Phys. U.S.S.R. 8, 253 (1944).

11. M. A. Biondi and S. C. Brown, Phys. Rev. 75, 1700 (1949)
    W. P. Allis and D. J. Rose, ibid. 93, 84 (1954)
    I. B. Bernstein and T. Holstein, ibid. 94, 1475 (1954).

12. The breakdown voltage pulses are adjusted in strength (keeping the duration fixed at ~7 μsec and repeated at 31.2 cycles per second) just enough to maintain a stable, repeatable, pulsed discharge. In this manner, the excitation light is usually very dim.

13. D. R. Bates, Editor, Atomic and Molecular Processes (Academic Press, New York, 1962).

14. W. P. Allis, Handbuch der Physik Volume XXI (Springer-Verlag, Berlin, 1956).

15. L. B. Loeb, Basic Processes in Gaseous Electronics (University of California Press, Berkeley, 1955), Chap. 1.
M. A. Biondi and L. M. Chanin, Phys. Rev. 122, 843 (1961).

16. R. H. Dicke, Rev. Sci. Instr. 17, 268 (1946).

17. D. Formato and A. Gilardini, Proceedings of the Fourth International Conference on Ionization Phenomena in Gases, Uppsala, 17-21 August, 1959 (North-Holland Publishing Company, Amsterdam, 1960, Edited by N. R. Nilsson), Vol 1, p. 99.

18. M. A. Biondi, Phys. Rev. 90, 730 (1953).

19. From Eqs (1) and (2), it can easily be shown that $\nu_{eff} = \frac{4}{3} N_m \bar{Q}_m \langle v \rangle$, where $\bar{Q}_m$ is the effective momentum transfer cross section and $\langle v \rangle = (8kT_e/\pi m)^{\frac{1}{2}}$. Then the effective momentum transfer collision probability $\bar{P}_m$ is given by $\bar{P}_m = \frac{3}{4} \frac{\nu_{eff}}{\langle v \rangle}$.

20. L. Gould and S. C. Brown, Phys. Rev. 95, 897 (1954);
J. L. Pack and A. V. Phelps, ibid. 121, 798 (1961).

21. J. L. Pack, R. E. Voshall and A. V. Phelps, Phys. Rev. 127, 798 (1962).

22. T. F. O'Malley, Phys. Rev. (to be published).

23. T. F. O'Malley, L. Spruch and L. Rosenberg, J. Math. Phys. 2, 491 (1961).
T. F. O'Malley, L. Spruch and L. Rosenberg, Phys. Rev. 125, 1300 (1962).

24. C. Ramsauer and R. Kollath, Ann. der Physik 12, 837 (1932).

25. P. Langevin, Ann Chim. et Phys. 5, 245 (1905).

26. A. A. Maryott and F. Buckley, Table of Dielectric Constants and Electric Dipole Moments of Substances in the Gaseous State (National Bureau of Standards Circular 537, 1953).

27. H. S. W. Massey and E. H. S. Burhop, Electronic and Ionic Impact Phenomena (Oxford at the Clarendon Press, 1952), Chap. 7.

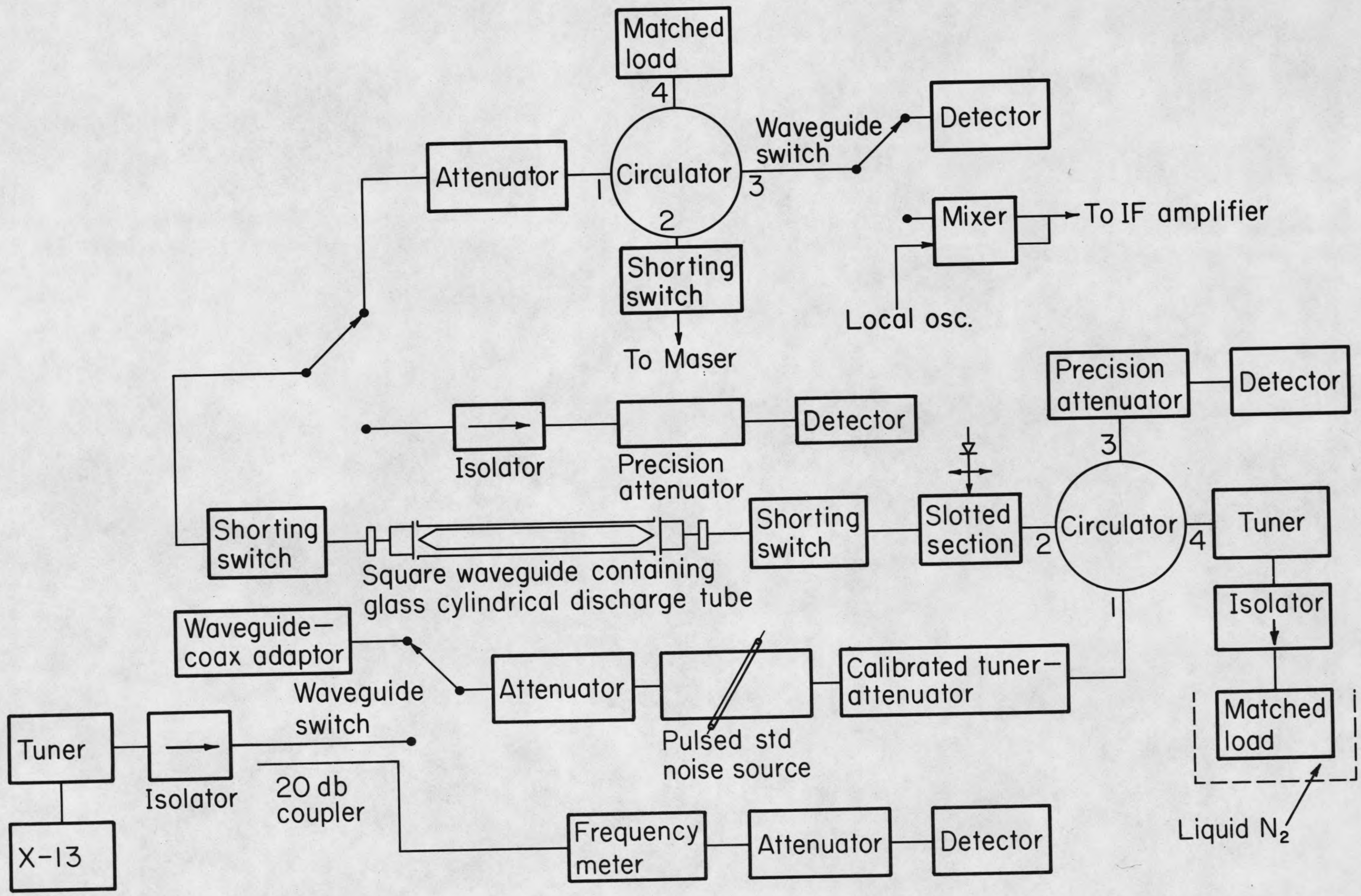

Microwave Instrumentation

Figure 1. Schematic diagram of one of the microwave circuitries employed in the present experiment.

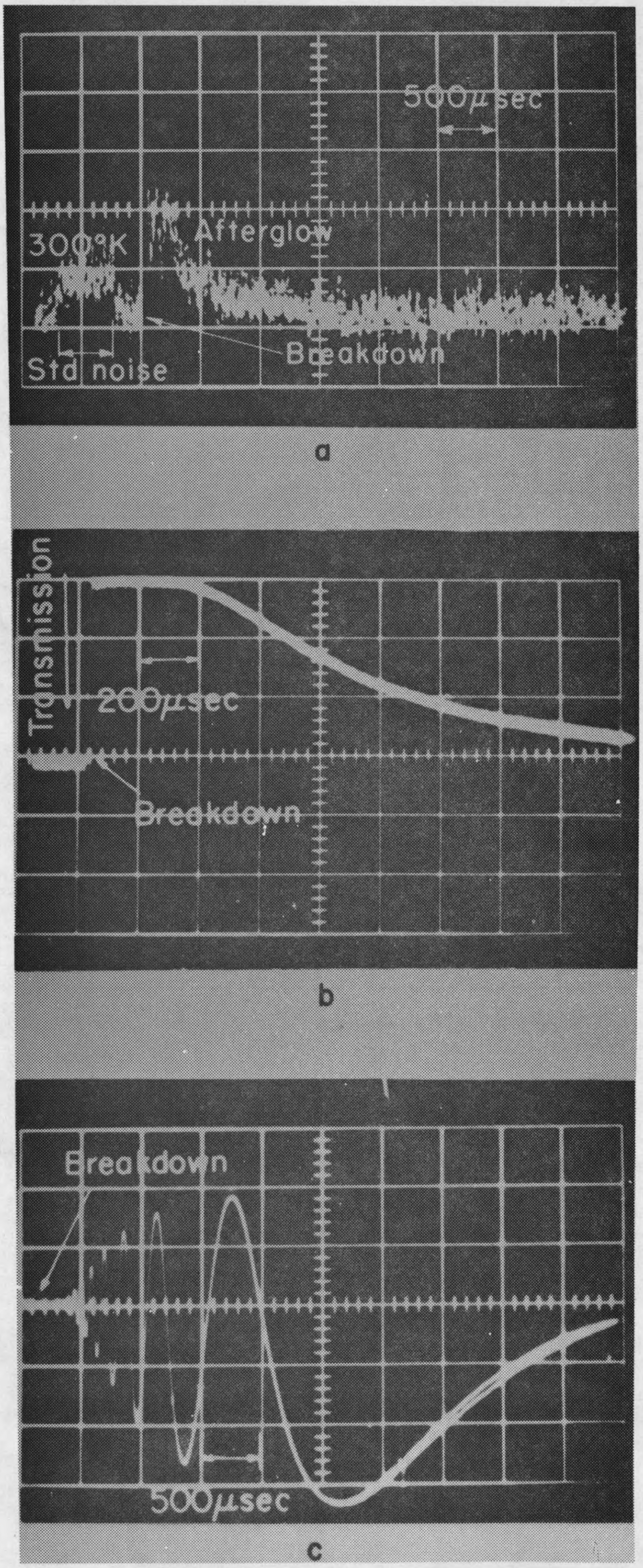

Figure 2. Noise and microwave measurements in He-Xe mixture of 54.6% Xe and a total pressure of 4.83 mmHg. (a) Direct comparison of the noise emitted by the decaying plasma with that from a standard noise source of 300°K. (b) Microwave signal (8.53 kMc/sec) transmitted through the decaying plasma. (c) Microwave interferometer trace.

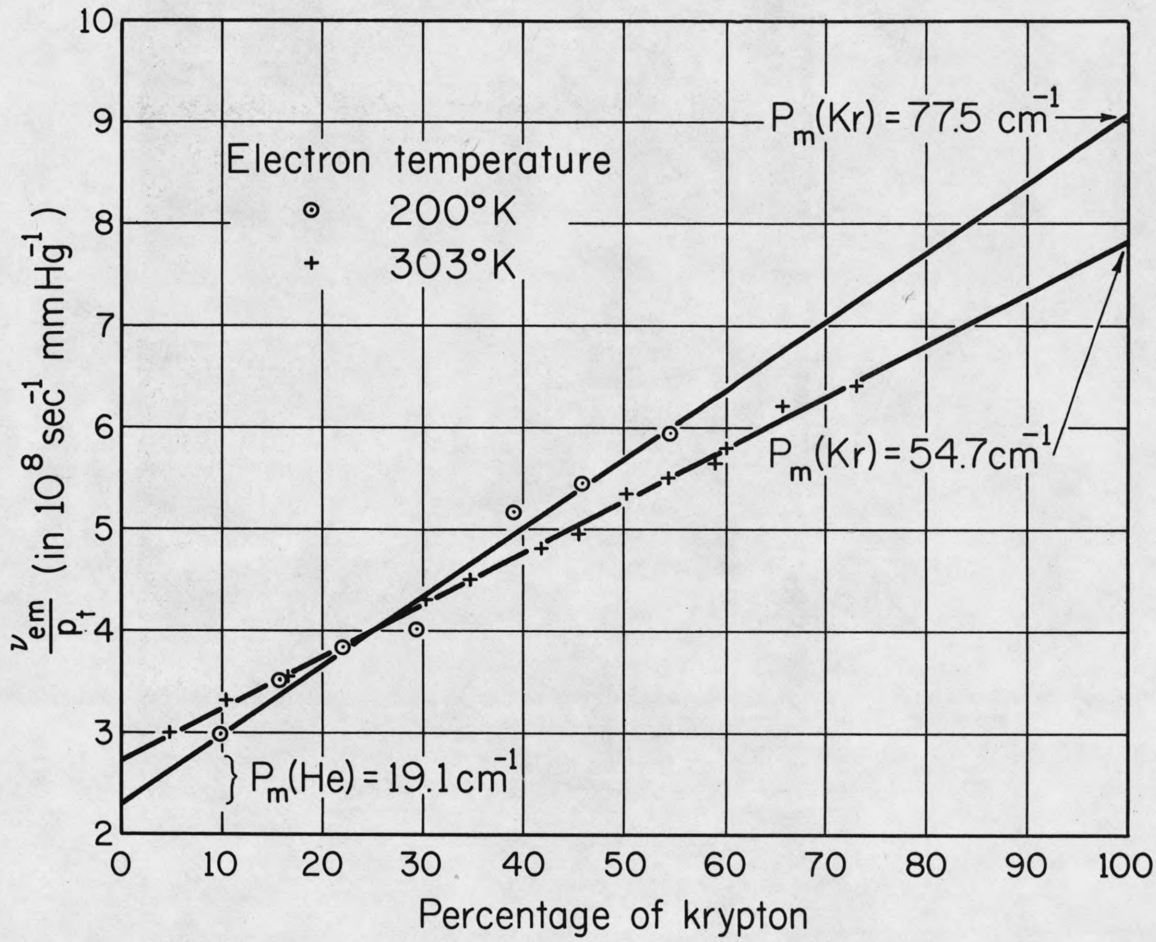

Figure 3. ν_{em}/p_t versus percentage of krypton in helium-krypton mixtures at 200 and 303°K. The straight line behavior is predicted by Eq (6) in the text under the condition of $(\frac{\nu}{\omega})^2 \ll 1$. The two ordinates of ν_{em}/p_t at 0 and 100% Kr give $\nu_{em}(He)/p(He)$ and $\nu_{em}(Kr)/p(Kr)$ at the temperatures indicated.

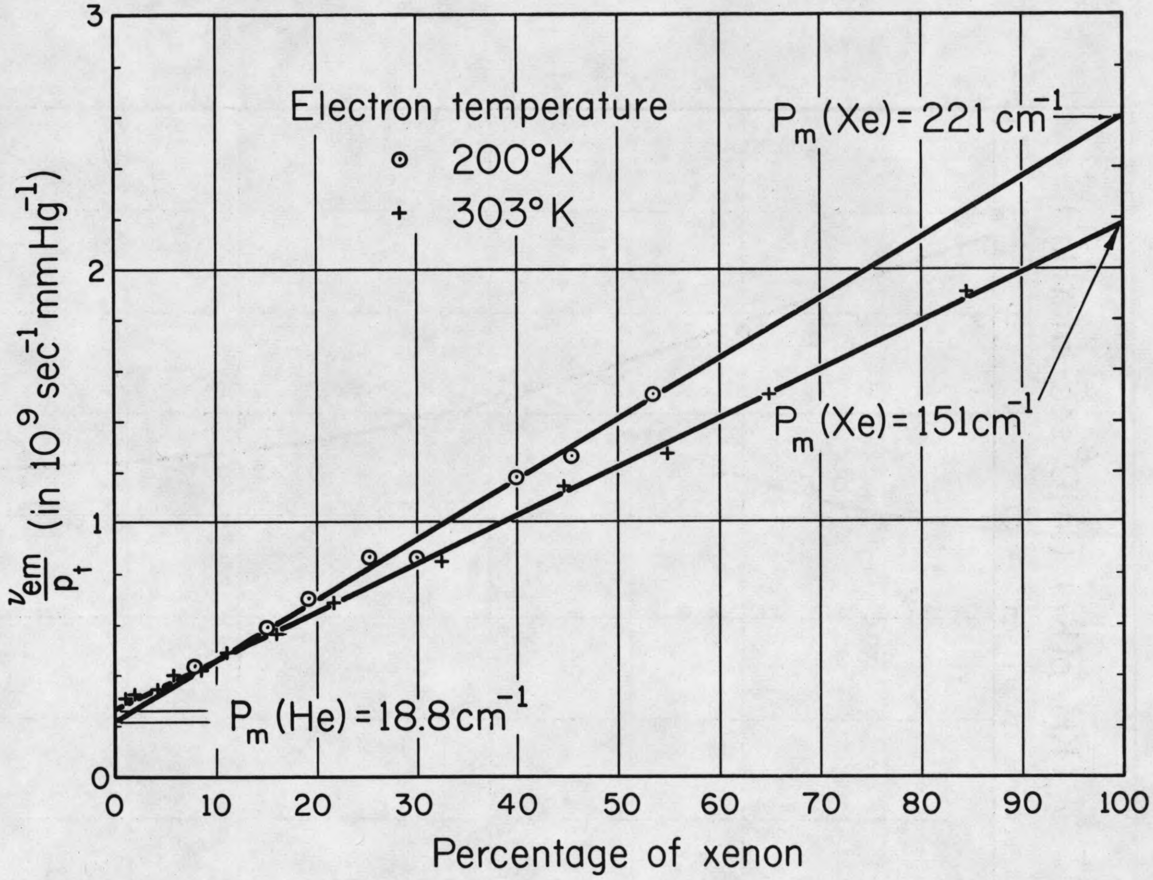

Figure 4. ν_{em}/p_t versus percentage of xenon in helium-xenon mixtures at 200 and 303°K. The straight line behavior is predicted by Eq (6) in the text under the condition of $(\frac{\nu}{\omega})^2 \ll 1$. The two ordinates of ν_{em}/p_t at 0 and 100% Xe give $\nu_{em}(He)/p(He)$ and $\nu_{em}(Xe)/p(Xe)$ at the temperatures indicated.

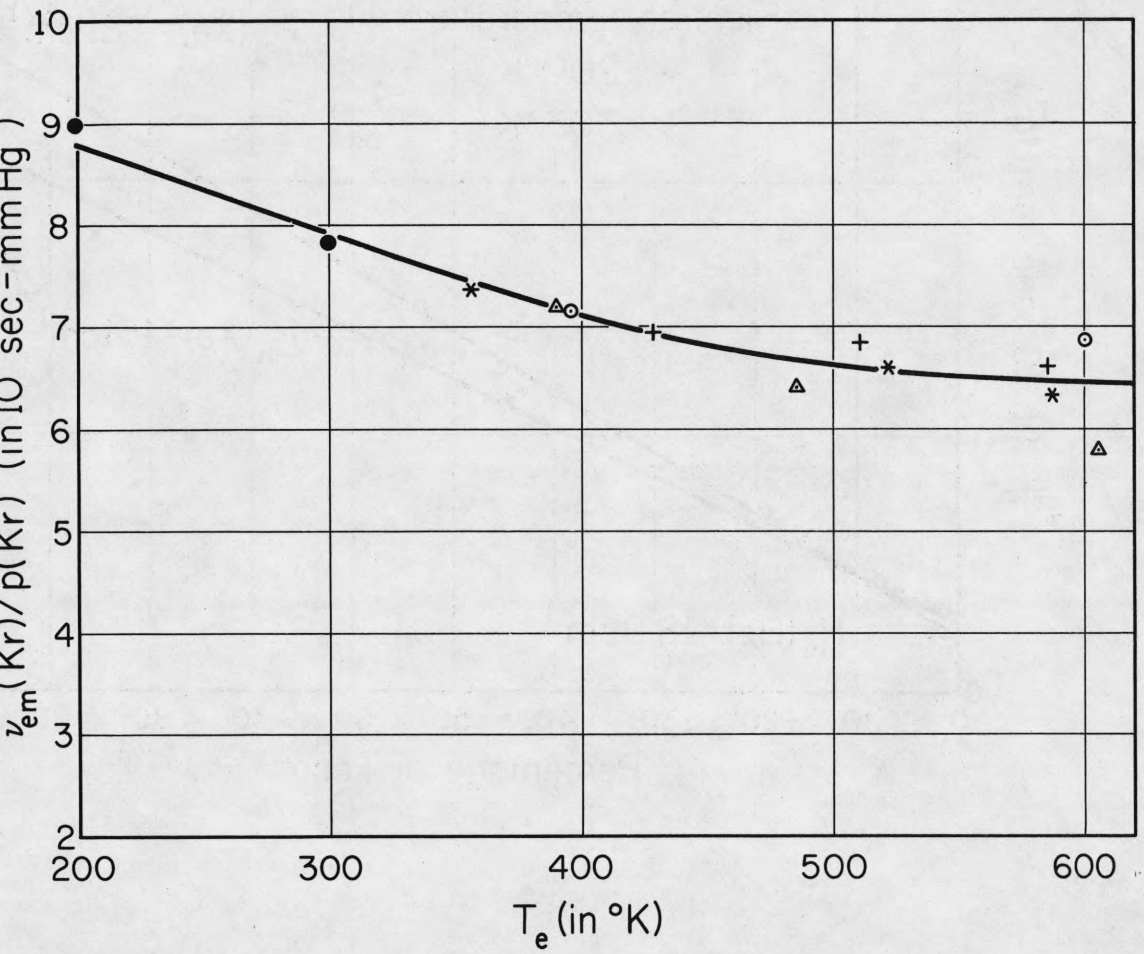

Figure 5. $\nu_{em}(Kr)/p(Kr)$ versus T_e. The various symbols on the graph represent the values of $\nu_{em}(Kr)/p(Kr)$ deduced from different fractional krypton concentrations: • from Fig. 3, * 41.6% Kr, ⊙ 50.1% Kr, + 58.8% Kr, Δ 73% Kr. The solid curve is the best fit to the experimental points according to Eq (4) and assuming $Q_m(v) = A + Bv + Cv^2$.

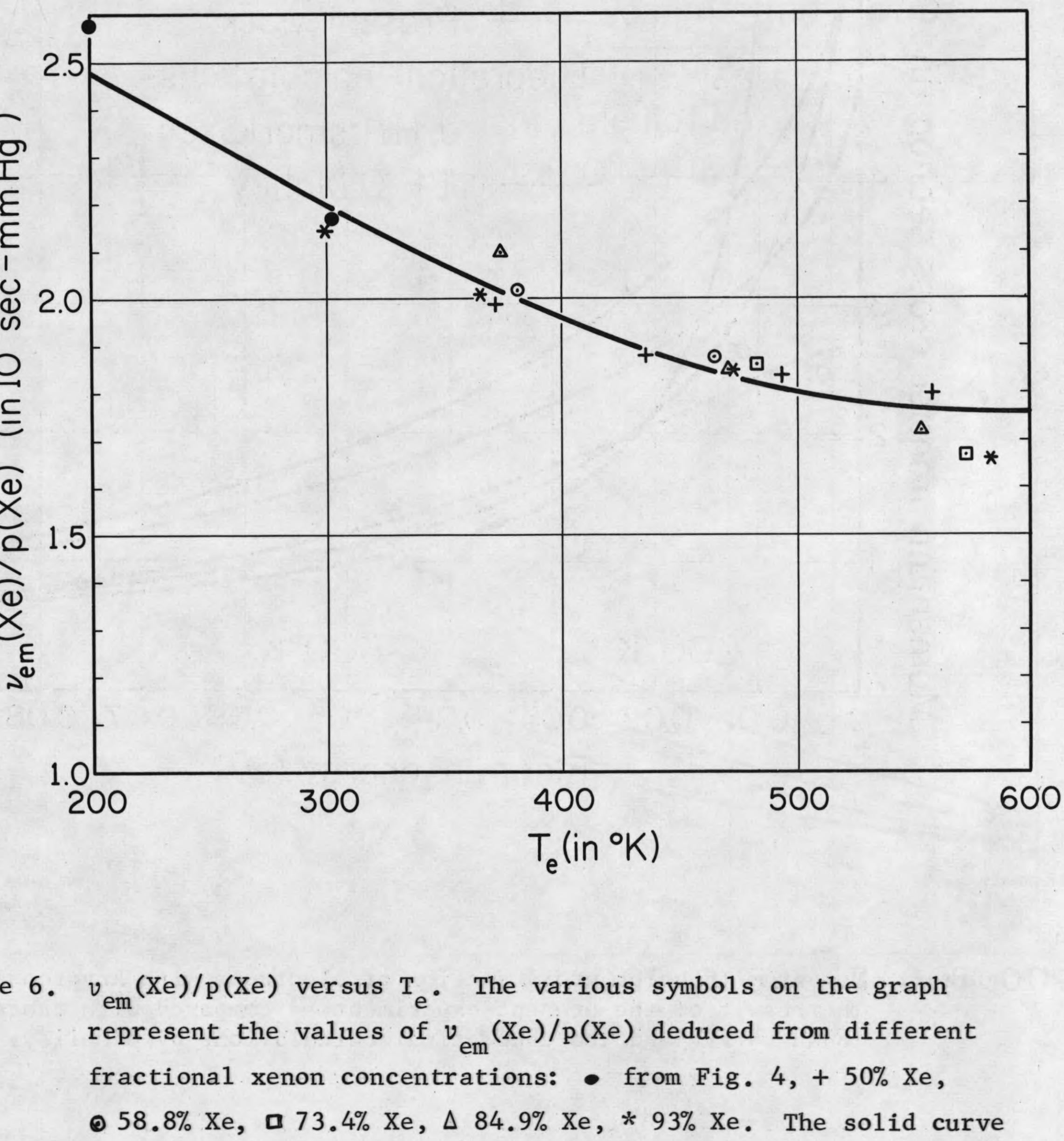

Figure 6. $\nu_{em}(Xe)/p(Xe)$ versus T_e. The various symbols on the graph represent the values of $\nu_{em}(Xe)/p(Xe)$ deduced from different fractional xenon concentrations: • from Fig. 4, + 50% Xe, ⊙ 58.8% Xe, ◻ 73.4% Xe, Δ 84.9% Xe, * 93% Xe. The solid curve is the best fit to the experimental points according to Eq (4) and assuming $Q_m(v) = A + Bv + Cv^2$.

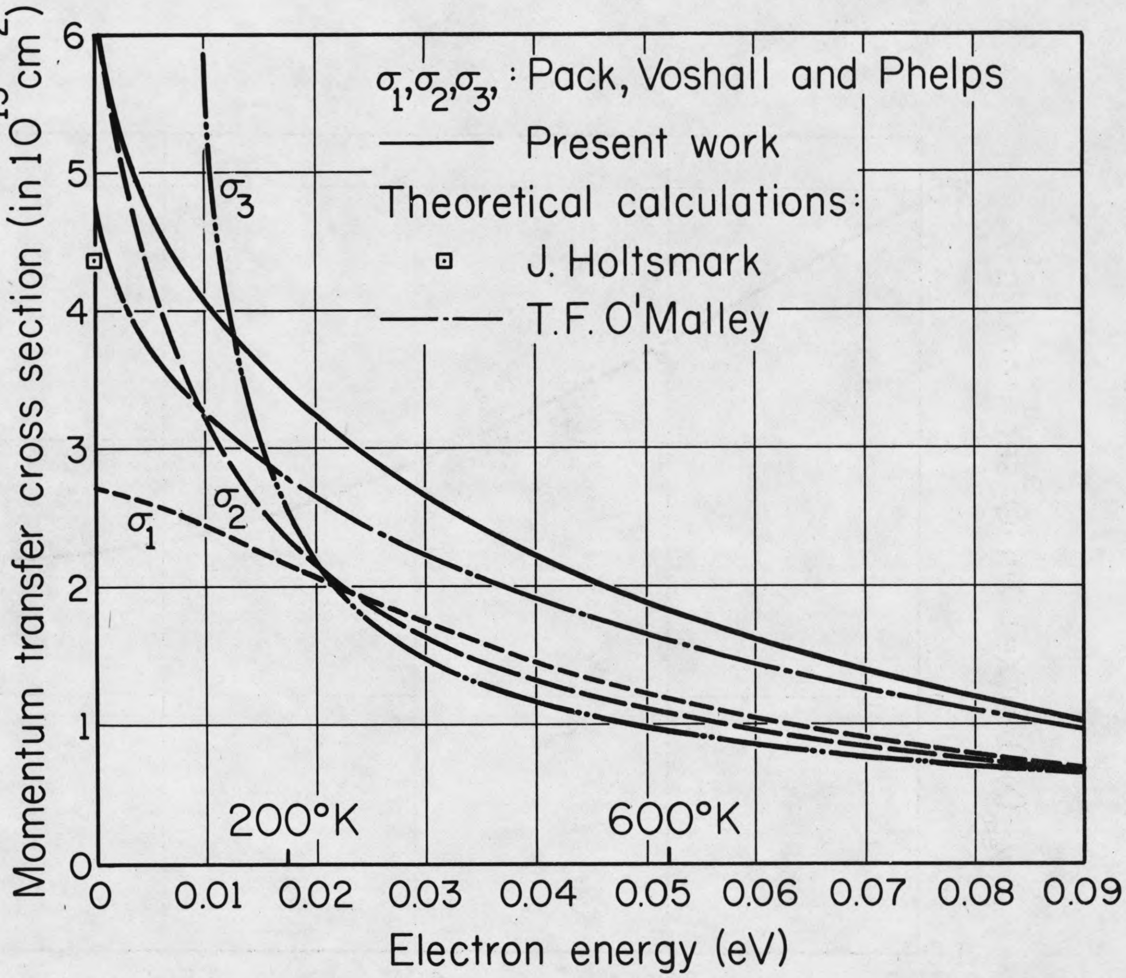

Figure 7. Momentum transfer cross section of electrons with krypton atoms. The result of the present experiment is compared with those found by PVP and the theoretical calculations by O'Malley.

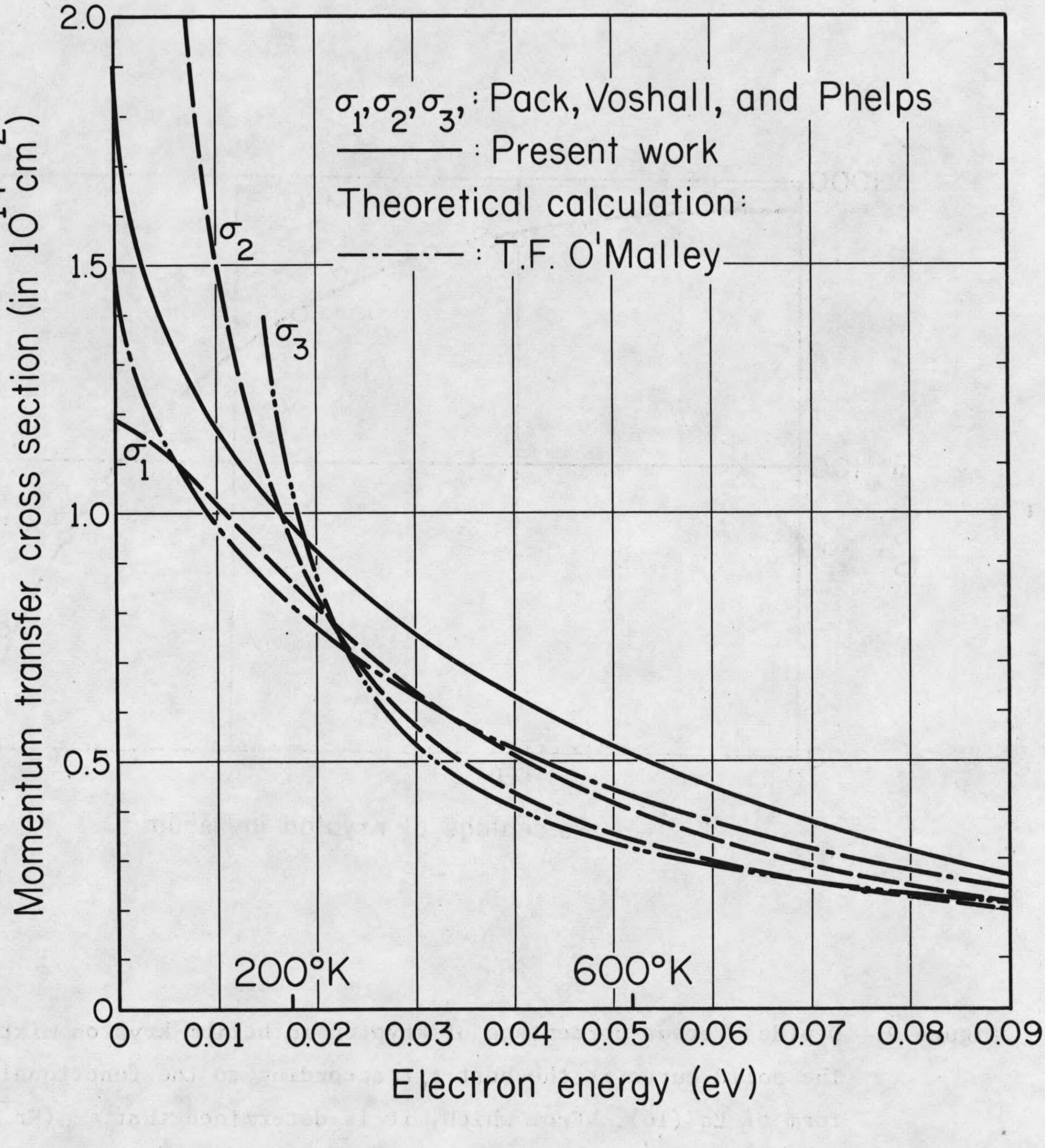

Figure 8. Momentum transfer cross section of electrons with xenon atoms. The result of the present experiment is compared with those found by PVP and the theoretical calculations by O'Malley.

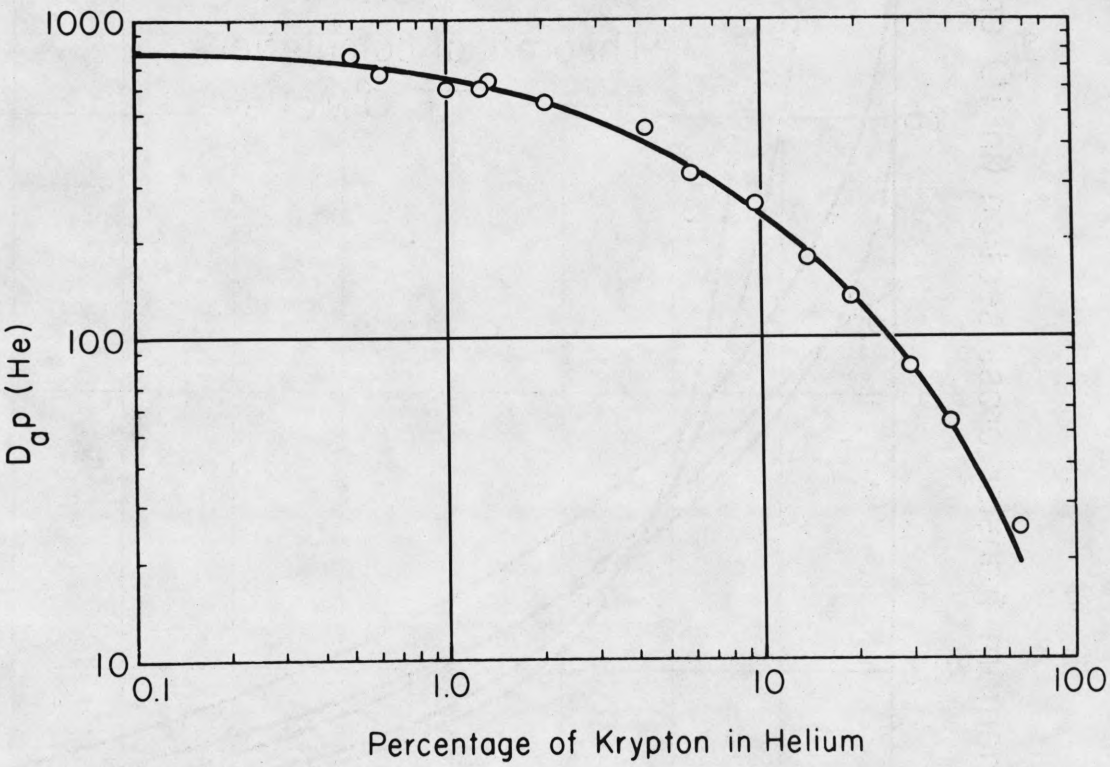

Figure 9. $D_a p$(He) versus percentage of krypton in helium-krypton mixtures. The solid curve is the best fit according to the functional form of Eq (16). From which, it is determined that: $\mu(Kr^+$ in He) $= 20.2 \pm 1.2$ cm^2/volt-sec and $\mu(Kr^+$ in Kr) $= 1.01 \pm 0.06$.

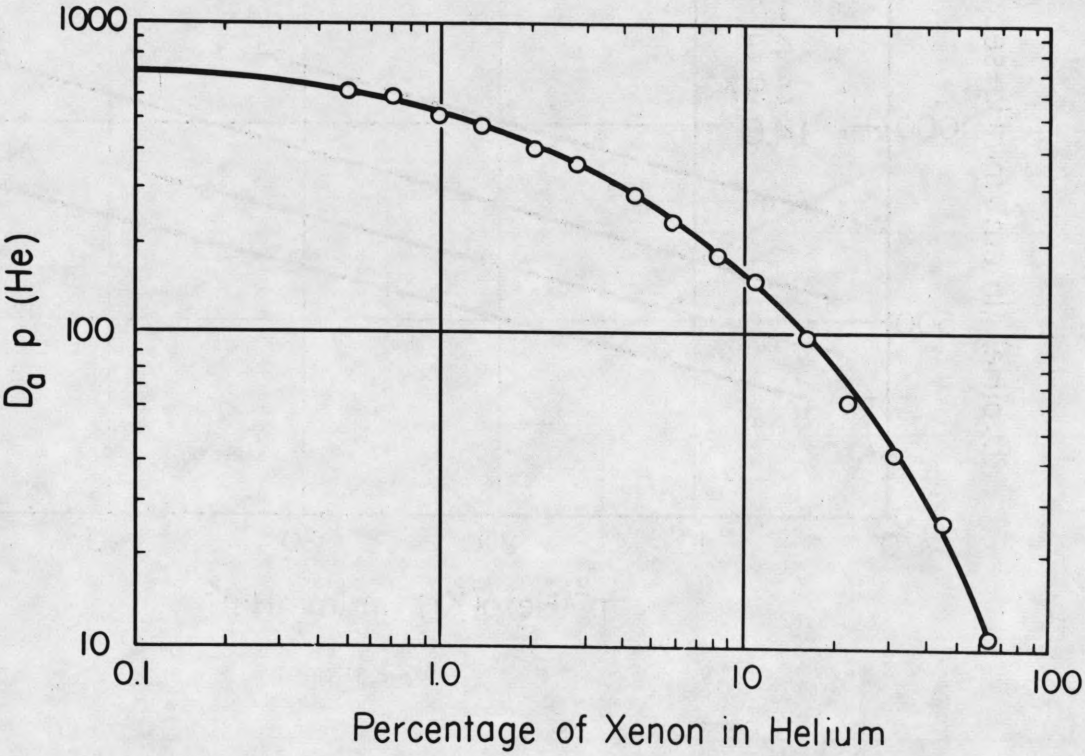

Figure 10. $D_a p$(He) versus percentage of xenon in helium-xenon mixtures. The solid curve is the best fit according to the functional form of Eq (16). From which, it is determined that: $\mu(Xe^+$ in He) = 18 $\pm$ 1.1 cm^2/volt-sec and $\mu(Xe^+$ in Xe) = 0.55 $\pm$ 0.03.

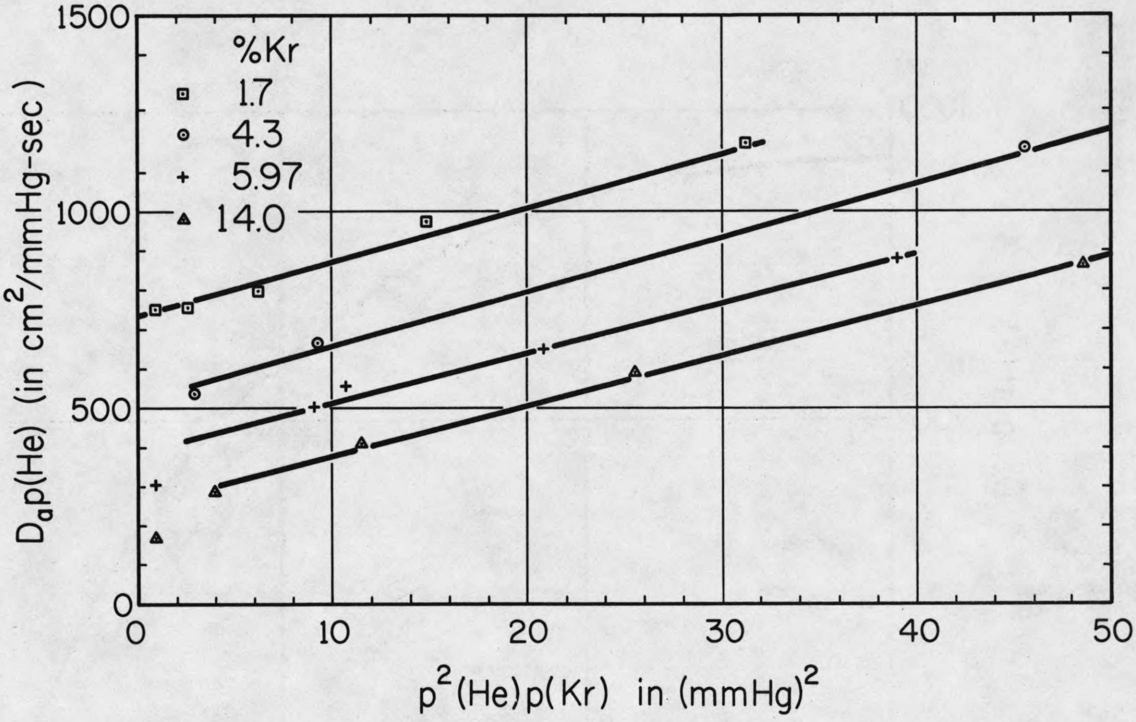

Figure 11. $D_a p(He)$ versus $p^2(He)p(Kr)$. The slope of which is proportional to the conversion frequency reaction (7).

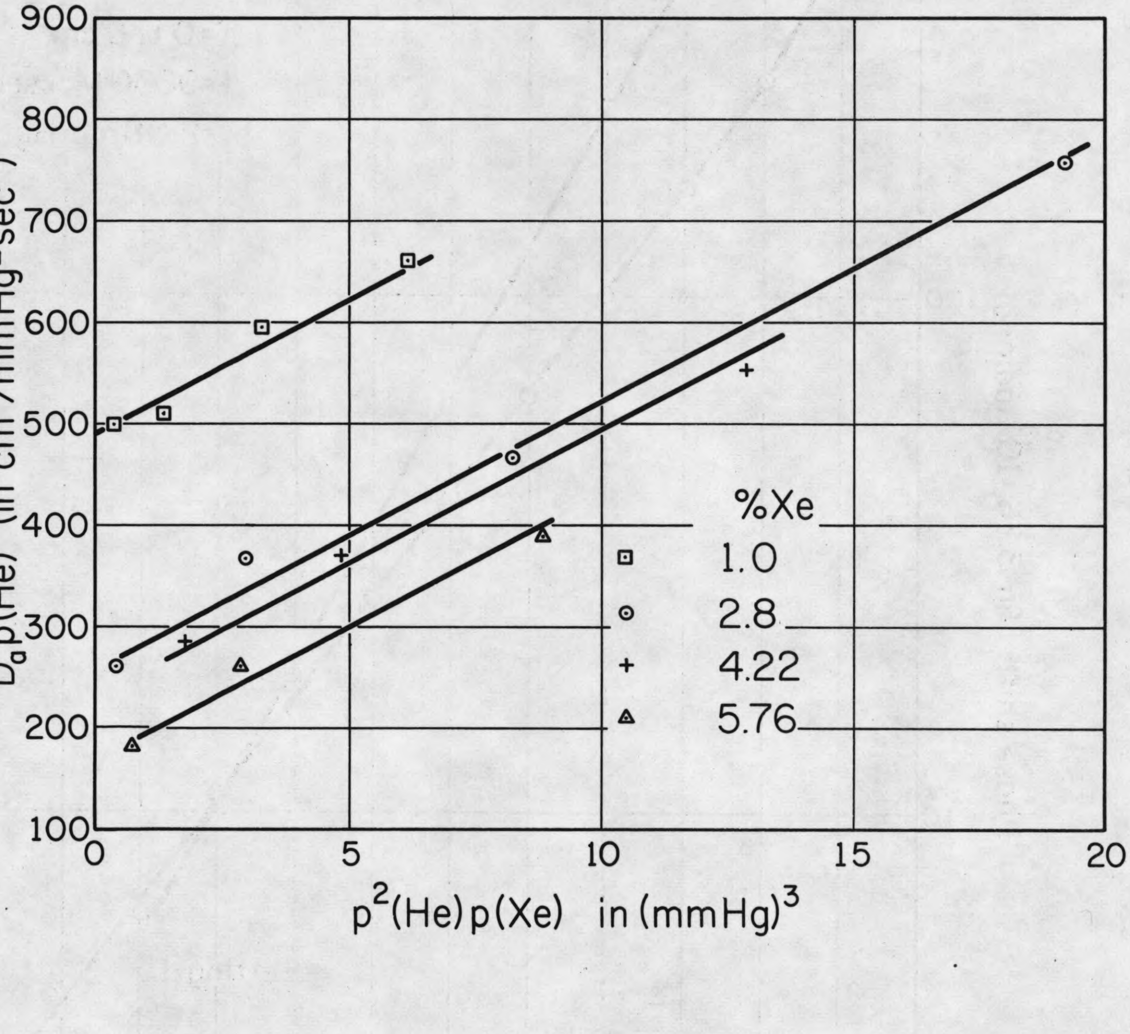

Figure 12. $D_a p(He)$ versus $p^2(He)p(Xe)$. The slope of which is proportional to the conversion frequency of reaction (7).

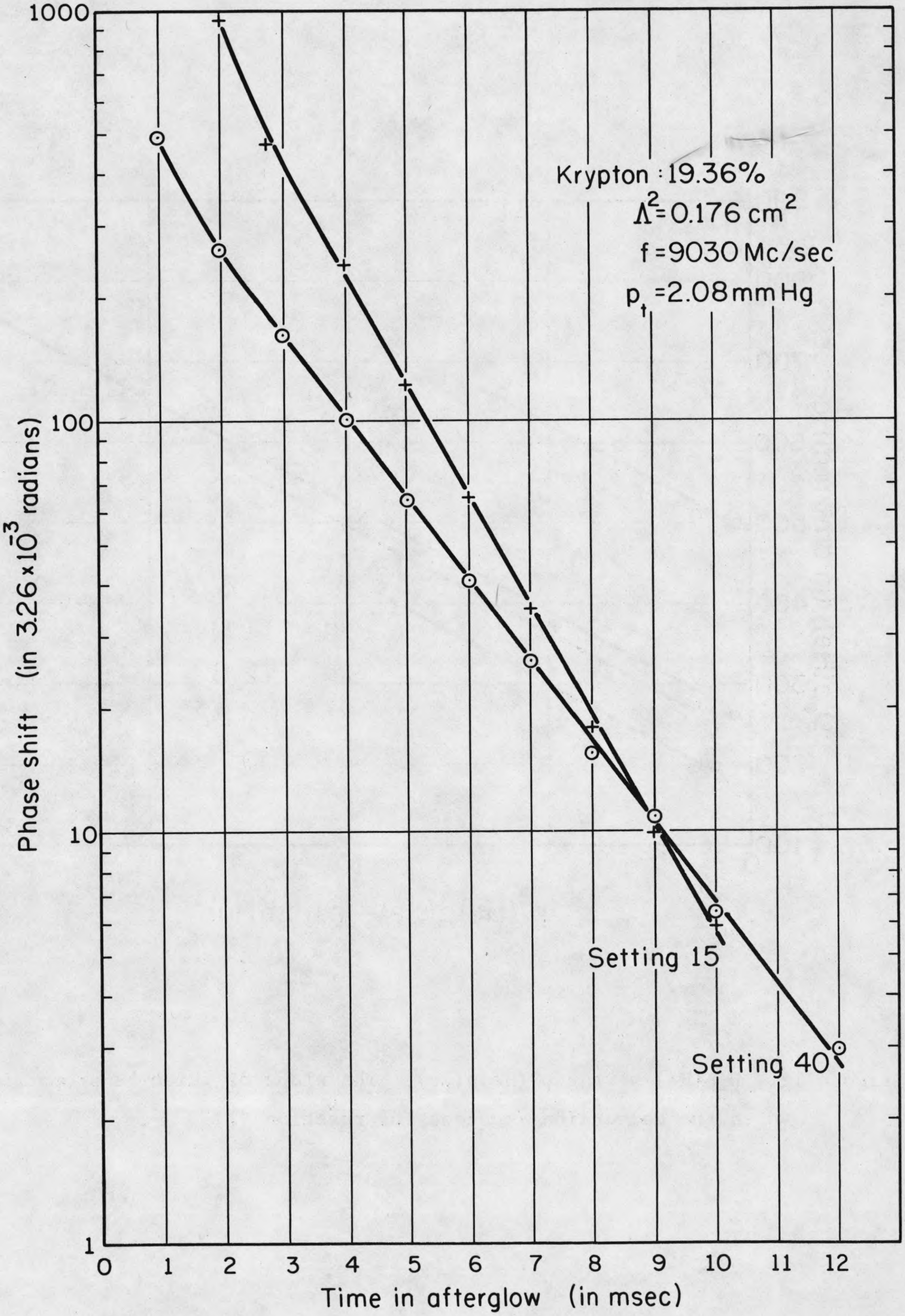

Figure 13. Electron density decay for two different breakdown voltage strengths in helium-krypton mixtures. The settings indicate the relative strength.

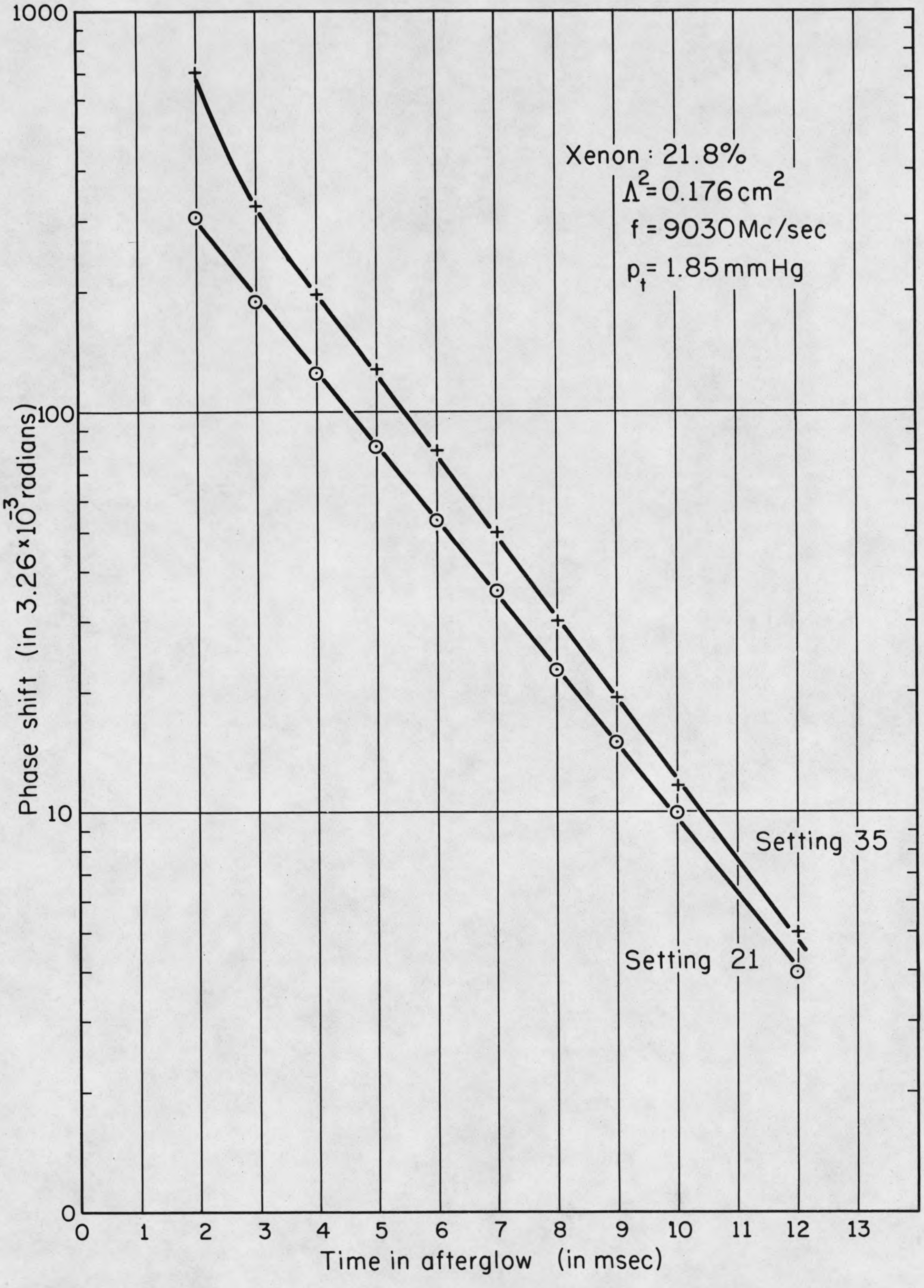

Figure 14. Electron density decay fro two different breakdown voltage strengths in helium-xenon mixtures. The settings indicate the relative strength.

DISTRIBUTION LIST AS OF NOVEMBER 7, 1962

1 Director
Air University Library
Maxwell Air Force Base, Alabama
Attn: CR-4803a

1 Redstone Scientific Information Center
U.S. Army Missile Command
Redstone Arsenal, Alabama

2 Hughes Aircraft Company
Florence and Teale
Culver City, California
Attn: N.E. Devereux
Technical Document Center

3 Autonetics
9150 East Imperial Highway
Downey, California
Attn: Tech. Library, 3041-11

1 Dr. Arnold T. Nordsieck
General Motors Corporation
Defense Research Laboratories
6767 Hollister Avenue
Goleta, California

1 Inspector of Naval Material
Los Angeles, California
Transmittal to:
Litton Systems, Inc.
5500 Canoga Avenue
Woodland Hills, California
Attn: Engineering Library

1 Sylvania Electronic Systems - West
Electronic Defense Laboratories
P. O. Box 205
Mountain View, California
Attn: Documents Center

1 Varian Associates
611 Hansen Way
Palo Alto, California
Attn: Dr. Ira Weissman

1 Huston Denslow
Library Supervisor
Jet Propulsion Laboratory
California Institute of Technology
Pasadena, California

1 Space Technology Labs, Inc.
One Space Park
Redondo Beach, California
Attn: Acquisitions Group
STL Technical Library

2 Commanding Officer and Director
U.S. Naval Electronics Laboratory
San Diego 52, California
Attn: Code 2800, C.S. Manning

1 Commanding Officer and Director
U.S. Navy Electronics Laboratory
San Diego 52, California
Attn: Library

1 Office of Naval Research Branch Office
1000 Geary Street
San Francisco, California

1 Stanford Electronics Laboratories
Stanford University
Stanford, California
Attn: SEL Documents Librarian

1 AFRST - SC
Headquarters, USAF
Washington 25, D. C.

1 Director of Science and Technology
Headquarters, USAF
Washington 25, D. C.
Attn: AFRST-EL/GU

1 Headquarters, R & T Division
Bolling Air Force Base
Washington 25, D. C.
Attn: RTHR

1 Headquarters, U.S. Army Materiel Command
Research Division, R & D Directorate
Washington 25, D. C.
Attn: Physics & Electronics Branch
Electronics Section

1 Commanding Officer
Diamond Ordnance Fuze Laboratories
Washington 25, D. C.
Attn: Librarian, Room 211, Bldg. 92

1 Operations Evaluation Group
Office of the CNO (Op03EG)
Navy Department
Washington 25, D.C.

1 Chief of Naval Operations
Tech. Analysis & Advisory Group (OP-07T)
Pentagon
Washington 25, D. C.

1 Commanding Officer & Director
David W. Taylor Model Basin
Navy Department
Washington 7, D. C.
Attn: Code 142, Library

1 Bureau of Ships
Department of the Navy
Washington 25, D. C.
Attn: Code 686

1 Bureau of Ships
Navy Department
Washington 25, D.C.
Attn: Code 732

1 Technical Library, DLI-3
Bureau of Naval Weapons
Department of the Navy
Washington 25, D. C.

1 Director
Naval Research Laboratory
Washington 25, D.C.
Attn: Code 5140

1 Department of the Navy
Office of Naval Research
Washington 25, D.C.
Attn: Code 437

1 Dr. H. Wallace Sinaiko
Institute for Defense Analyses
Research & Engineering Support Division
1666 Connecticut Ave., N.W.
Washington 9, D.C.

1 Data Processing Systems Division
National Bureau of Standards
Conn. at Van Ness
Room 239, Bldg. 10
Washington 25, D.C.
Attn: A.K. Smilow

1 Exchange and Gift Division
The Library of Congress
Washington 25, D.C.

1 NASA Headquarters
Office of Applications
400 Maryland Avenue, S.W.
Washington 25, D.C.
Attn: Mr. A. M. Greg Andrus
Code FC

1 APGC (PGAPI)
Eglin Air Force Base
Florida

1 Martin Company
P.O. Box 5837
Orlando, Florida
Attn: Engineering Library
MP-30

1 Commanding Officer
Office of Naval Research, Chicago Branch
John Crerar Library Building
10th Floor, 86 East Randolph Street
Chicago 1, Illinois

1 Librarian
School of Electrical Engineering
Purdue University
Lafayette, Indiana

2 Keats A. Pullen, Jr.
Ballistic Research Laboratories
Aberdeen Proving Ground, Maryland

1 Research Analysis Corporation
6935 Arlington Road
Bethesda 14, Maryland
Attn: Library

5 Scientific & Technical Information Facility
P. O. Box 5700
Bethesda, Maryland
Attn: NASA Representative (S-AK/DL)

1 Commander
Air Force Cambridge Research Laboratories
Laurence G. Hanscom Field
Bedford, Massachusetts
Attn: CRXL

1 Research Laboratory of Electronics
Massachusetts Institute of Technology
Cambridge 39, Massachusetts
Attn: Document Room, 26-327

1 Lincoln Laboratory
Massachusetts Institute of Technology
P.O. Box 73
Lexington 73, Massachusetts
Attn: Library, A-082

1 Sylvania Electric Products Inc.
Electronic Systems
Waltham Labs. Library
100 First Avenue
Waltham 54, Massachusetts

1 Minneapolis-Honeywell Regulator Co.
Aeronautical Division
2600 Ridgeway Road
Minneapolis 13, Minnesota
Attn: Mr. D. F. Elwell
Main Station: 625

1 Inspector of Naval Material
Bureau of Ships Technical Representative
1902 West Minnehaha Avenue
St. Paul 4, Minnesota

20 Activity Supply Officer
Building 2504
Charles Wood Area
Fort Monmouth, New Jersey
Marked: For Office of Engineering Operations
Order No. 39578-PM-60-91-91

1 Radio Corporation of America
RCA Laboratories
David Sarnoff Research Center
Princeton, New Jersey
Attn: Library

1 Dr. J. H. Frank
861 Washington Avenue
Westwood, New Jersey

1 Mr. A. A. Lundstrom
Bell Telephone Laboratories
Room 2E-127
Whippany Road
Whippany, New Jersey

1 AFMDC (MDSGP/Capt. Wright)
Holloman Air Force Base
New Mexico

1 Mailing Zone C-57
Bell Aerosystems Company
P. O. Box 1
Buffalo 5, New York
Attn: Technical Library

1 Cornell Aeronautical Laboratory, Inc.
4455 Genesee Street
Buffalo 21, New York
Attn: J. P. Desmond, Librarian

1 Sperry Gyroscope Company
Marine Division Library
155 Glen Cove Road
Carle Place, L.I., New York
Attn: Mrs. Barbara Judd

1 Rome Air Development Center
Griffiss Air Force Base, New York
Attn: Documents Library
RAALD

1 General Electric Company
Advanced Electronics Center
Cornell University
Ithaca, New York
Attn: F. Kuehn, Librarian

1 Library
Light Military Electronics Department
General Electric Company
Building No. 28-501
Schenectady 5, New York

3 Commanding Officer
U.S. Army Research Office (Durham)
Attn: CRD-AA-IP, Mr. Ulsh
Box CM, Duke Station
Durham, North Carolina

1 Goodyear Aircraft Corporation
For: Project MX 778
Akron 15, Ohio

1 Battelle-DEFENDER
Battelle Memorial Institute
505 King Avenue
Columbus 1, Ohio

1 ASD (ASNC)
Wright-Patterson Air Force Base
Ohio

1 ASD (ASRNG)
Wright-Patterson Air Force Base
Ohio

1 Commanding Officer (AD-5)
U.S. Naval Air Development Center
Johnsville, Pennsylvania
Attn: NADC Library

2 Commanding Officer
Frankford Arsenal
Philadelphia 37, Pennsylvania
Attn: SMUFA-1300

1 General Atronics Corporation
1075 DeHaven Street
West Conshohocken, Pennsylvania
Attn: Miss D. M. Keener
Librarian

1 H. E. Cochran
Oak Ridge National Laboratory
P. O. Box X
Oak Ridge, Tennessee

1 President
U.S. Army Air Defense Board
Fort Bliss, Texas

1 U.S. Air Force Security Service
San Antonio, Texas
Attn: ODC-R

1 ASTIA Technical Library AFL 2824
Arlington Hall Station
Arlington 12, Virginia
Attn: TISLL

1 U.S. Naval Weapons Laboratory
Computation and Analysis Laboratory
Dahlgren, Virginia
Attn: Mr. Ralph A. Niemann

2 Army Materiel Command
Research Division
R & D Directorate
Bldg. T-7
Gravelley Point, Virginia